Microstructure of the nitrogen pair in crystalline silicon studied by ion channeling

F. Berg Rasmussen and B. Bech Nielsen
Institute of Physics and Astronomy, University of Aarhus, DK-8000 Århus C, Denmark
(Received 27 December 1993; revised manuscript received 7 March 1994)

The structure of the nitrogen pair in crystalline silicon has been studied by the channeling technique and by infrared absorption spectroscopy. Silicon crystals have been implanted with ^{15}N at room temperature and have subsequently been annealed at 725 °C to form pairs. The channeling measurements have been carried out at 136 K using the nuclear reaction $^{15}N(p,\alpha)^{12}C$ to probe the ^{15}N atoms, and the angular distribution of the α particle yield has been measured around all major crystal axes and planes. The major part of the implanted nitrogen atoms (70%) is found to occupy a unique type of site which is displaced by 1.1 Å from a perfect lattice site along a ⟨100⟩ direction. The population of this type of site has the same annealing properties as the local vibrational modes associated with the nitrogen pair in silicon. The experimental findings are consistent with a recently suggested model of the nitrogen pair.

I. INTRODUCTION

In contrast to other group-V elements nitrogen is an ineffective donor in silicon, and its equilibrium solid solubility is two or three orders of magnitude below those of other important impurities such as phosphorus, boron, carbon, and oxygen.[1-3] In spite of this, nitrogen has gained technological interest due to its ability to suppress swirl defects and to lock dislocations in silicon.[4] However, the origins of these effects as well as the microstructures of several important nitrogen-related defects in silicon remain unknown.

Infrared absorption measurements[5,6] on nitrogen-implanted samples revealed local vibrational modes of nitrogen with frequencies in the range from 600 to 1000 cm^{-1}. Especially two modes at 766 and 963 cm^{-1} observed in ^{14}N-implanted material are prominent and have the same annealing behavior.[7] In the case of ^{15}N implantation the two modes shift down to 749 and 937 cm^{-1} and implantation of ^{14}N and ^{15}N into overlapping profiles gives rise to two additional modes at 759 and 947 cm^{-1}. From this Stein[8] concluded that these modes originate from a pair of nitrogen atoms bonded to silicon atoms.

The nitrogen pair is also the dominant defect observed by infrared absorption in silicon crystals doped with nitrogen during growth.[9] A detailed insight into the physical properties of this defect is therefore essential for the understanding of nitrogen in silicon. However, this requires that the microstructure of the defect is known. The present paper addresses this problem.

If the nitrogen atoms forming the pair were inequivalent, four new modes should appear in samples implanted with both ^{14}N and ^{15}N, but only two were observed. This indicates that the two nitrogen atoms are equivalent. Although this was not stated explicitly by Stein, he did propose[10] three models having this property (see Fig. 1): (a) pairing on adjacent lattice sites, (b) a ⟨100⟩-oriented nitrogen pair in a vacancy, and (c) bonding between adjacent nitrogen atoms on Si-Si bridge bonds. In the first model the nitrogen atoms are expected

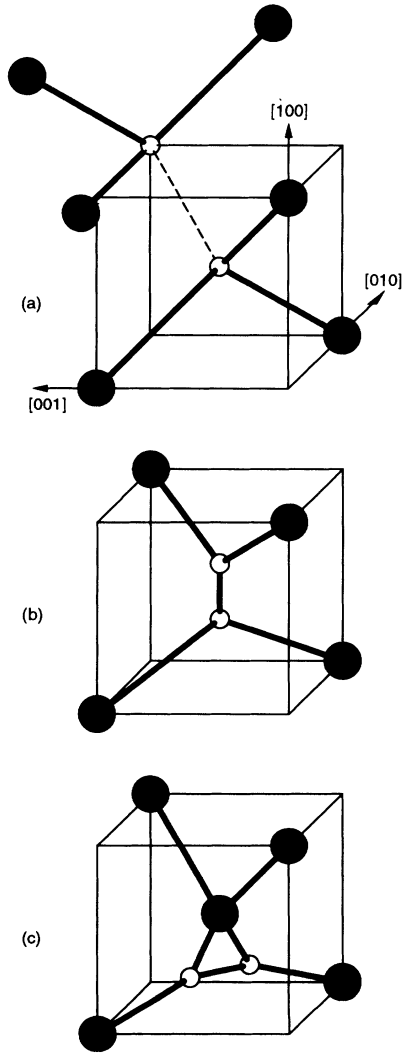

FIG. 1. Three models of the nitrogen pair defect in silicon proposed by Stein (Ref. 10). (a) A N pair on adjacent Si sites, (b) a ⟨100⟩-oriented N pair in a vacancy, or (c) two N atoms on Si-Si bridge bonds.

to be essentially threefold coordinated with a Si-N bond length of ~ 1.7 Å, which is typical for silicon nitride (Si_3N_4) and various molecular compounds, e.g., trisilylamine $(SiH_3)_3N$.[11] Thus this structure should have a large N-N separation distance and the nitrogen atoms should be located somewhere between a substitutional site (S) and an antibonding site (AB) (see Fig. 2). In the second model a N-N bond is formed with an expected bond length of $\sim 1.5-1.6$ Å, characteristic for a molecular N-N bond.[12] In this case the nitrogen position will be close to a Z site (see Fig. 2), while the third model predicts a position close to a bond-center (BC) site (see Fig. 2). Thus the lattice location of the nitrogen atoms will distinguish between these models.

The lattice location of the nitrogen atoms may be determined by a channeling experiment. This type of experiment does not distinguish between equivalent sites. As the paired nitrogen atoms are equivalent, a channeling study should therefore lead to a unique type of site, an ideal situation for such an experiment. A previous channeling study by Mitchell *et al.*[13] on ^{15}N-implanted Si showed that less than 5% of the implanted nitrogen may occupy a substitutional site, but no specific site was identified. In the present work, the channeling technique has been applied to determine the lattice location of paired nitrogen in silicon. The site identified is inconceivable with all the above-mentioned models. An alternative model was recently suggested[14] which consists of two neighboring ⟨100⟩-oriented Si-N split interstitials, arranged in an antiparallel configuration and with four Si-N bonds forming a square lying on a {110} plane. This "antiparallel" model is consistent with the experimental findings presented here, previous infrared absorption measurements, and *ab initio* theory.

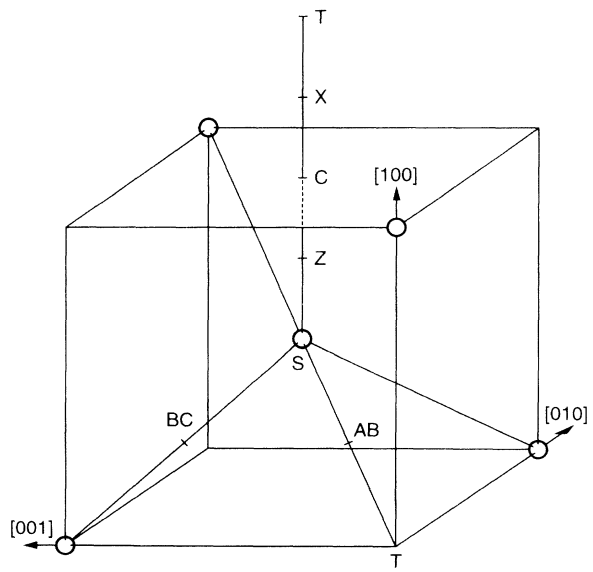

FIG. 2. Various impurity sites in the silicon lattice; substitutional (S), bond-center (BC), antibonding (AB), tetrahedral (T), Z, C, and X sites.

II. EXPERIMENTAL DETAILS

A. Sample preparation

Float-zone silicon wafers with the surface normal to a ⟨100⟩, ⟨110⟩, or ⟨111⟩ crystal axis and with thickness of about 350 μm were cut in squares of $\approx 12\times 12$ mm^2. The wafer material was p type with boron concentrations ranging from 6×10^{13} to 3×10^{16} cm^{-3}, and the concentration of other impurities was quoted to be less than 10^{16} cm^{-3}. Most samples were polished on one side only but the samples used in the annealing study (see below) were polished on both sides.

The samples were implanted at room temperature with $^{15}N^+$ ions using a 600-keV accelerator equipped with a universal ion source and a large magnet for mass separation. The normal of the samples was tilted 7° off the beam direction to avoid channeling effects, and the beam was horizontally and vertically swept in order to ensure a homogeneous lateral distribution over the sample. The implanted dose was determined from the current measured on the sample which was surrounded by a shield biased to -300 V to reduce the effect of secondary electrons. The absolute uncertainty on the implanted dose is about 5%.

Most samples were implanted on one side only at various energies and doses as stated in Table I. This resulted in a nearly uniform profile with 6.5×10^{19} N/cm^3 extending from 0.12 to 0.55 μm below the surface. The samples used in the annealing study were implanted on both sides and to a greater depth, 0.82 μm (see Table II), in order to increase the infrared absorption from the nitrogen impurities.

A series of preliminary infrared absorption measurements showed that a 5-sec rapid thermal anneal (RTA) at 725 °C resulted in maximum absorption from the nitrogen pair and in the disappearance of all other nitrogen-related modes. Consequently all samples were subjected to this annealing treatment unless otherwise stated. Finally the surface oxide was removed by a HF etch.

B. Infrared absorption measurements

After the samples had been prepared, infrared absorption measurements were carried out at room temperature with a Nicolet System 800, Fourier-transform spectrometer equipped with a HgCdTe (MCT) detector and a Ge-KBr beam splitter. The number of scans was typically 200, boxcar apodization was applied, and the apodized resolution was 3.8 cm^{-1} as determined from the full width at half maximum of the modes around 1500 cm^{-1} due to water vapor.

The samples used in the annealing study were preannealed at 600 °C only and the intensities of the nitrogen pair lines were found to be identical in all samples. Sub-

TABLE I. Energies and doses used in the ^{15}N implantations.

Energy (keV)	50	90	150	225
Dose (cm^{-2})	5.0×10^{14}	7.0×10^{14}	9.0×10^{14}	1.3×10^{15}

TABLE II. Energies and doses used for the samples in the annealing experiment.

Energy (keV)	50	90	150	225	325	400
Dose (10^{14} cm^{-1})	5.0	7.0	9.0	10.0	9.0	11.0

sequently these samples were RTA annealed at different temperatures between 700 and 950 °C for 5 sec and the infrared absorption spectra were measured again.

C. Channeling measurements

The channeling method and the experimental setup have been described previously[15,16] and only a brief account will be given here. The sample was placed in a computer-controlled motor-driven x-y goniometer with an angular resolution of 0.01°. The goniometer was mounted in a vacuum chamber pumped to a pressure below 3×10^{-6} Torr. The sample was cooled to 136 K and kept at that temperature during measurement. Moreover, the target was surrounded by an electrically insulated cryoshield held at $\approx$120 K to reduce surface contamination on the target.

The channeling measurements were carried out with a 1015-keV proton beam supplied by a HVEC 2-MV Van de Graaff accelerator. The beam was collimated by two slits 3 m apart, each set at 1×1 mm^2, resulting in a beam divergence of about 0.02°. The implanted ^{15}N atoms were probed by means of the nuclear reaction ^{15}N$(p,\alpha)^{12}$C, detecting the ~4-MeV α particles in a large-area (4.9 cm^2) solid-state detector placed at an angle of about 135° relative to the beam direction at a distance of 3.5 cm from the sample. In front of this detector a ~2-μm-thick aluminum foil was placed which stopped the major part of the protons backscattered from the silicon host and hence severe dead-time problems were avoided. As shown in Fig. 3 the α particles and the high-energy tail of the backscattered protons could be well separated. The backscattered protons were monitored with another solid-state detector (scattering angle ~135°) with a very small acceptance angle and the proton yield was integrated over a depth interval corresponding to the range of the implanted nitrogen.

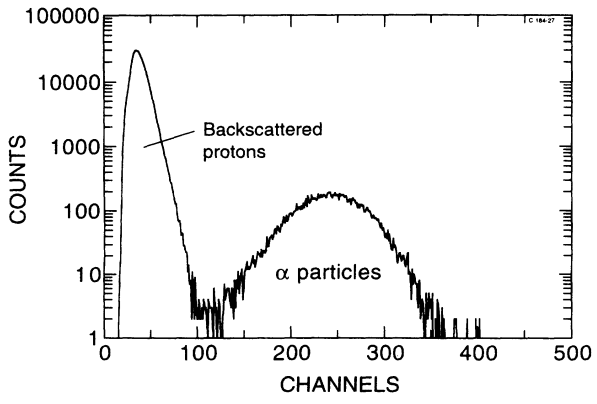

FIG. 3. Spectrum measured by the α detector with the beam incident in a random direction.

The proton energy was chosen so that the cross section for the nuclear reaction was constant to within 5% over the nitrogen depth profile.[17] Although the stopping power of the analyzing beam may have varied by a factor of ~2 when the beam was scanned through an axis, this corresponds only to a less than 2% variation in the integrated α-yield cross section over the implanted region.

For a fixed beam fluence the α-particle and proton yields were measured simultaneously as a function of the tilt angle, i.e., the angle between the beam and the crystal axis or plane. These angular distributions were measured for all major axes and planes. The fluence for each data point was 2.5 μC and the beam current was 1–10 nA measured on the target with the cryoshield biased to −400 V.

In the axial case the yield at each tilt angle was measured as an average over all azimuthal angles.[16] This procedure results in a reliable yield at large tilt angles (random yield) used to normalize all the data, improves the reproducibility of the angular distributions, and makes the quantitative comparison between experimental distributions and simulations based on the continuum model meaningful.[16,18] The angular distributions across the planes were measured with the angle Θ between the beam and a nearby major axis being fixed. In each case Θ was carefully selected to avoid channeling effects from high-index axes, which show up clearly in the variation of the proton yield when Θ is scanned with the beam parallel to the plane. The values of Θ applied were between 6° and 9°. Also, the planar yields were normalized to the random yield, which in this case was determined as the average yield in a measurement extending about 20° on each side of the plane, starting and ending at the center of other planes. In order to reduce the effect of beam-induced radiation damage, the data points were always measured in a sequence going from the center of the axis or plane toward larger tilt angles.

D. Channeling simulation

The lattice location was determined from a comparison of the experimental angular distributions with the results of computer simulations[16] corresponding to different nitrogen sites. The simulations are based on the continuum model[18] with the assumption of statistical equilibrium on a transverse energy shell,[18] modified to take dechanneling in the perfect lattice into account.[16,19] The thermal vibrations of both the impurity and the host atoms are included in the simulation. The two-dimensional vibrational amplitude of the host atoms was assumed to be 0.072 Å as estimated from a Debye model,[20] whereas the vibrational amplitude of the impurity was used as a fitting parameter.[21] This simulation scheme has been successfully applied in several lattice location experiments.[16,22,23] It has been shown to reproduce experimental results[24] and to give results similar to Monte Carlo simulations.[25] The details of the simulations have been described elsewhere.[16,24]

III. RESULTS

A. Channeling experiments on samples annealed at 725°C

The experimental α-particle angular distributions around the major axes are shown in Fig. 4 together with simulations corresponding to the sites illustrated in Fig. 2. The vibrational amplitude of the impurity is in this case assumed to be equal to that of the host atoms. The measured distribution in α-particle yield around the $\langle 100 \rangle$ axis has a sharp peak superimposed on a broader dip. The broad dip is consistent only with a position located at or very close to the line segment connecting a substitutional (S) site with the nearest interstitial tetrahedral (T) site in a $\langle 100 \rangle$ direction. The experimental $\langle 100 \rangle$ distribution is qualitatively consistent with the simulated curve for the C site, located halfway between the S and T sites. As the position is displaced from the C site toward the Z or X site (see Figs. 2 and 4), the central peak decreases and finally transforms into a small and narrow dip. The peak height is hence a sensitive measure of the displacement from the C site. The same conclusion may be drawn from the $\langle 111 \rangle$ experimental distribution. The Z and X sites are rather similar and may be distinguished only from the $\langle 110 \rangle$ axial and the $\{111\}$ planar distributions. The $\langle 110 \rangle$ distribution shows a dip which is consistent with a nitrogen position between Z and C sites but is inconsistent with a position between X and C sites. Consequently, it may be concluded that a substantial part of the nitrogen atoms is located between neighboring Z and C sites.

A detailed analysis has been performed to obtain the site giving the best possible fit to the data. This best fit is shown in Figs. 5 and 6 as solid lines together with the experimental points for all major axes and planes and a nice overall agreement is observed. The fit is obtained with 70 ± 6 % of the nitrogen atoms displaced 1.1 ± 0.1 Å from substitutional sites along $\langle 100 \rangle$ directions and with the rest of the nitrogen atoms being randomly located. The maximum displacement of the dominant site perpendicular to the axis is 0.2 Å and the two-dimensional vibrational amplitude is 0.24 ± 0.04 Å. The uncertainties represent conservative estimates and they were determined from a visual comparison of the experimental data with the simulated curves calculated for various displacements, vibrational amplitudes, and populations of the site.

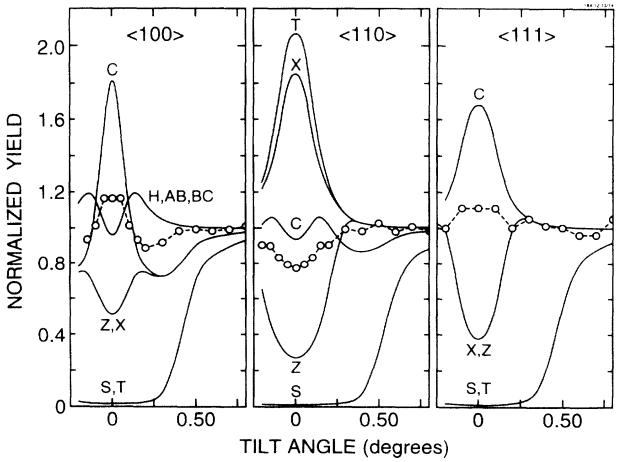

FIG. 4. Measured angular distribution in α-particle yield (○) after annealing at 725 °C shown for the three major axes together with simulations (solid lines) corresponding to the sites shown in Fig. 2. The dashed lines are drawn to guide the eye.

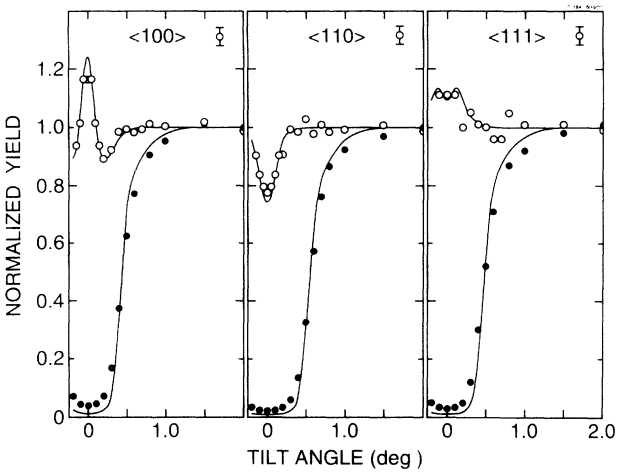

FIG. 5. Measured axial angular distribution in α-particle yield (○) after annealing at 725 °C shown together with the best fit to all of the data (solid line). Also shown is the axial angular distribution in proton yield (●) and the simulated distribution corresponding to a substitutional lattice site.

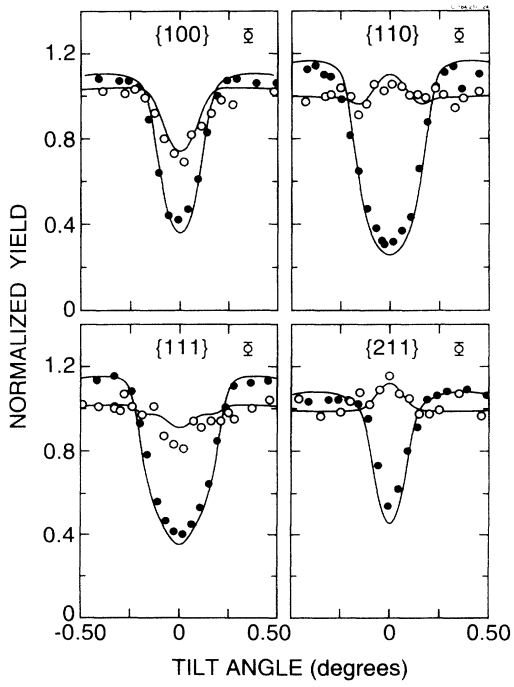

FIG. 6. Measured planar angular distributions in α-particle yield (○) after annealing at 725 °C shown together with the best fit to the data (solid line). Also shown is the measured planar angular distributions in proton yield (●) and the simulated distribution corresponding to a substitutional lattice site.

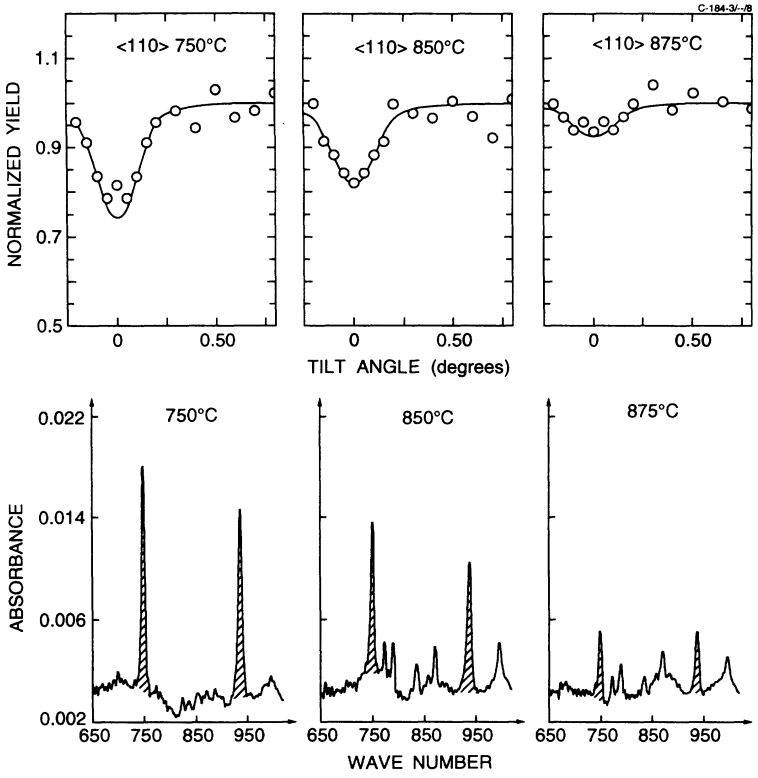

FIG. 7. Effect of annealing on the ⟨110⟩-channeling data (upper part) and the infrared absorption spectrum (lower part). The open circles are the experimentally measured angular distribution in α-particle yield and the solid lines are the best fit obtained with the ⟨100⟩-displaced site and a random component (see the text). The infrared absorption lines corresponding to the pair defect have been hatched for clarity.

B. Isochronal annealing study

The effects of RTA treatment at 600 °C and subsequent annealing at 750, 850, or 875 °C on the infrared absorption and on the ⟨110⟩-channeling dip are shown in Fig. 7. The infrared absorbance spectra have been subtracted by a reference spectrum measured on samples annealed at 950 °C where all nitrogen-related modes have disappeared.

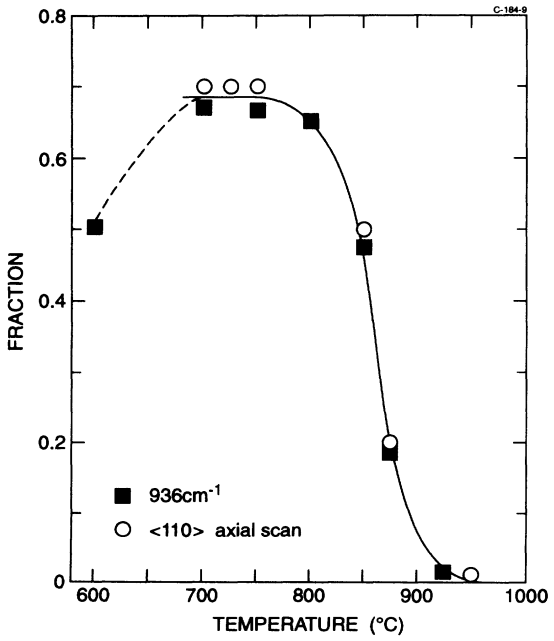

FIG. 8. Fraction of nitrogen atoms at the ⟨100⟩-displaced site identified by channeling (○) compared to the fraction of nitrogen present as pairs (■) as a function of annealing temperature. The line is drawn to guide the eye.

Assuming that all nitrogen atoms are located at the ⟨100⟩-displaced site or at a random position the ⟨110⟩ angular distributions in α-particle yield could be fitted at all annealing temperatures, simply by varying the population of the two components. The simulations shown in Fig. 7 correspond to a population of 70% at 750 °C, 50% at 850 °C, and 20% at 875 °C. It is apparent from the figure that the annealing of the nitrogen pair modes occurs parallel with the depopulation of the identified nitrogen site. In Fig. 8 the relative population of the ⟨100⟩-displaced site is compared with the fraction of nitrogen atoms present in the form of pairs as determined spectroscopically. The latter fraction was found from the peak height of the pair mode at 963 cm^{-1} using a published coefficient[26] (1.83×10^{17} cm^{-2}) and assuming a uniform nitrogen profile (6.5×10^{19} N/cm^3) of depth 0.70 μm on both sides of the samples. The ⟨100⟩ and {100} angular distributions were also measured as a function of annealing temperature and the results were in accordance with those for the ⟨110⟩ case.

IV. DISCUSSION

The implantation creates a large number of defects which gives rise to a significant increase in the normalized proton (or host) minimum yield $\chi^h_{\min}$. However, after annealing at 725 °C, $\chi^h_{\min}$ is only slightly larger than that for a virgin crystal, which indicates successful recrystallization of the samples as a result of this treatment. In the case of the ⟨110⟩ axis, $\chi^h_{\min}$ was 0.04 on the implanted

crystal and 0.03 on a virgin crystal. If this increase in $\chi^h_{\min}$ is ascribed to backscattering on randomly located silicon atoms, the fraction of these may be estimated to be 0.2 at. % in the implanted layer. This corresponds to one or two displaced silicon atoms per implanted nitrogen atom. Thus the increase in $\chi^h_{\min}$ may be associated with backscattering on silicon atoms which are directly involved in the nitrogen defects or alternatively are displaced by the stress field surrounding these defects.

A full measurement of the angular distribution around on axis led in itself to an increase of about 0.02 in $\chi^h_{\min}$, whereas the corresponding α yield was unchanged. Furthermore, on a few samples infrared absorption spectra were measured on spots irradiated during the channeling measurement and no changes in the pair-mode intensity nor any new features in the spectra were detected. Apparently the channeling measurement neither creates new infrared-active defects nor does it destroy existing nitrogen pairs. Defects created during the measurement may thus be disregarded in the interpretation of the nitrogen channeling data.

The decrease in the population of the ⟨100⟩-displaced site and the annealing of the pair defect are clearly correlated, as can be seen from Figs. 7 and 8. It might be argued that this does not necessarily imply that the identified site is associated with the pair defect. However, the relative population of the ⟨100⟩-displaced site agrees quantitatively with the fraction of nitrogen atoms present as pairs. In samples annealed at 725 °C this fraction is 70%, i.e., the pair modes observed by infrared absorption *and* the nitrogen position identified by channeling both correspond to the dominating nitrogen defect. On this basis it is concluded that the ⟨100⟩-displaced site is the location of the nitrogen atoms forming the pair defect.

The concentration of nitrogen is ~0.13 at. % and thus several orders of magnitude larger than that of other impurities, e.g., boron, carbon, and oxygen. The incorporation of other impurities in the pair defect can therefore be disregarded. This was also confirmed experimentally as no difference was observed between channeling data measured on *p*-type and *n*-type crystals of various resistivities. The pair defect may be a part of a large defect involving silicon vacancies and/or interstitials. However, the structure cannot be too complex since the same defect is observed in as-grown material and since $\chi^h_{\min}$ is low. Any influence of the orientation of the sample surface can also be neglected as the ⟨110⟩ angular distributions were measured on samples with different surface orientations and no changes in these distributions were observed.

The two-dimensional vibrational amplitude for nitrogen found in the channeling simulation (0.24±0.04 Å) is much larger than that of the host atoms (0.072 Å). This can be interpreted in two ways: Either the defect may possess a very low-frequency mode, about ~50 cm^{-1}, which gives rise to nitrogen vibrations with such a large amplitude. Or, what may seem more likely, the large vibrational amplitude may reflect minor differences in the actual positions of the nitrogen atoms. Such a distribution of nitrogen sites is expected to cause a broadening of the infrared absorption peaks. This could be the reason

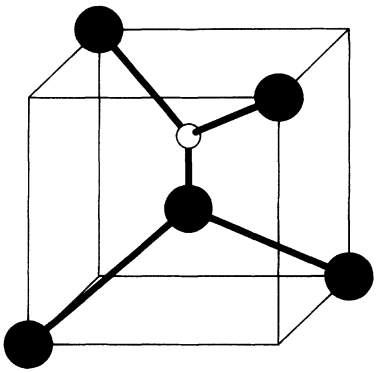

FIG. 9. ⟨100⟩-oriented Si-N split interstitial.

that the full widths at half maximum of the local vibrational modes are rather large, 6.3 cm^{-1} for the 748-cm^{-1} mode and 7.6 cm^{-1} for the 936-cm^{-1} mode.

The trigonal and bridge-bond models of Stein [Figs. 1(a) and 1(c)] may be ruled out immediately as they do not agree with the ⟨100⟩-displaced site, while the ⟨100⟩-oriented nitrogen pair in a vacancy (N_2-V) [Fig. 1(b)] agrees qualitatively with this site. However, for consistency the N-N bond length must be around 2.2 Å, which is much longer than the 1.5–1.6 Å expected on chemical grounds. Theoretical *ab initio* cluster calculations[14] found the N_2-V defect to be stable but with a bond length of only 1.5 Å, so clearly this model must be abandoned too. The calculations also showed that models involving a direct N-N bond in general were unable to reproduce the high-frequency infrared-active mode at 963 cm^{-1} (^{14}N), indicating that the nitrogen pair involves Si-N bonds only. Furthermore, the calculations[14] found that the interstitial nitrogen is a ⟨100⟩-oriented Si-N split interstitial as shown in Fig. 9 with a Si-N bond length (parallel to ⟨100⟩) of 1.74 Å and with the nitrogen atom displaced by 1.0 Å along ⟨100⟩ from the perfect lattice site. This position is *very* close to the position found for the nitrogen atoms in the pair, and based on this a different model of the pair was recently suggested.[14] This model consists of two neighboring Si-N split interstitials arranged in an antiparallel configuration and with four Si-N bonds forming a square lying on a {011} plane. The calculations found that the nitrogen atoms are displaced 1.1 Å from a substitutional site in a ⟨100⟩ direction and 0.2 Å perpendicular to this displacement (see Fig. 10). This position is *consistent* with the channeling

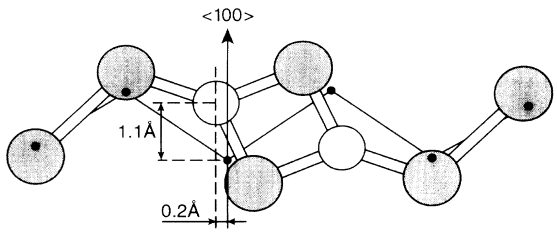

FIG. 10. Antiparallel model of the nitrogen pair defect (Ref. 14) shown in the (01$\bar{1}$) mirror plane (reproduced from Ref. 14). The small points mark the substitutional (perfect lattice) sites. Also indicated is the calculated (Ref. 14) displacement of the nitrogen atoms from the substitutional site.

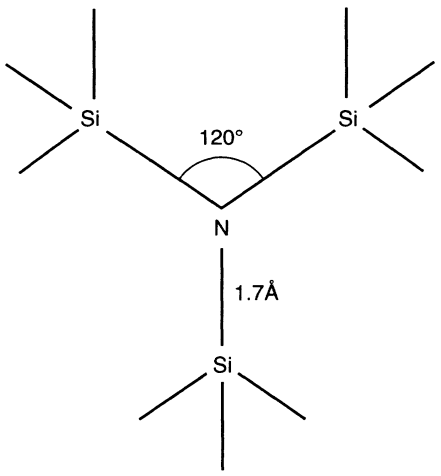

FIG. 11. Basic structure (Ref. 11) of, e.g., silicon nitride, showing the preferred bond length of 1.7 Å and bond angle of about 120°.

data. Moreover, the calculations[14] predicted two infrared-active local vibrational modes with frequencies and isotope shifts in agreement with experiment.

The antiparallel model of the nitrogen pair seems natural for several reasons. Simple compounds involving silicon and nitrogen, e.g., silicon nitride (Si_3N_4) or trisilylamine [$(SiH_3)_3N$], all show infrared absorption due to Si-N stretch vibrations in the range 950–1000 cm^{-1} (^{14}N), suggesting that the nitrogen pair in silicon essentially has the same structure as Si_3N_4 or $(SiH_3)_3N$. The basic structure of these compounds is shown in Fig. 11 and it is characterized by Si-N bond lengths close to 1.7 Å and Si-N bond angles close to 120°, i.e., bonding through sp^2-like orbitals on the nitrogen and sp^3-like orbitals on the silicon atoms. These bond lengths and types of bonding are retained in the antiparallel model. As noted by Stein[10] the low-frequency 766-cm^{-1} mode (^{14}N) must pertain to the structure of the nitrogen pair as no vibrational frequencies appear for the Si-N compounds in this frequency range. The origin of this mode has a simple explanation with the antiparallel model. The two Si-N interstitials forming the pair have bond lengths of ~1.7 Å,[14] which essentially are responsible for the high-frequency 963-cm^{-1} mode (^{14}N). However, the nearest-neighbor distance in silicon is 2.35 Å and this forces some of the Si-N bonds to be longer, as otherwise too much strain will be introduced in the lattice. A longer Si-N bond has a lower stretch frequency and this accounts for the 766-cm^{-1} mode. This simple physical picture is confirmed by the detailed calculations.[14] Finally, from a formation point of view a pair based on combination of two Si-N interstitials seems natural since the Si-N interstitials are expected to diffuse rather rapidly during annealing.

V. SUMMARY

The structure of the nitrogen pair in silicon has been studied by the channeling technique and by infrared absorption spectroscopy. The channeling measurements revealed a unique type of nitrogen site which is displaced 1.1±0.1 Å from a substitutional site along a ⟨100⟩ direction. After annealing at 725 °C the major part of the nitrogen atoms (70±6 %) was found to occupy such sites, while the remaining part was randomly distributed. The ⟨100⟩-displaced site has been shown to be the lattice location of nitrogen atoms forming the principal pair defect in silicon.

The channeling measurements and infrared experiments presented in this paper are all fully consistent with the antiparallel model of the nitrogen pair in silicon. In this model the nitrogen pair consists of two antiparallel Si-N interstitials bonded into a "squarelike" configuration with bond lengths closely resembling those found in Si-N molecular compounds.

Furthermore, *ab initio* calculations on this structure were able to reproduce the experimental findings. The combined agreement between theory and experiment represents strong support to the antiparallel model of the nitrogen pair in crystalline silicon.

ACKNOWLEDGMENTS

The authors wish to acknowledge R. Jones (University of Exeter) for numerous stimulating and helpful discussions. This work has been supported by the Danish Natural Science Research Council, Jr. No. 11-7961.

[1]P. V. Pavlov, E. I. Zorin, D. I. Tetelbaum, and A. F. Khoklov, Phys. Status Solidi A **35**, 11 (1976).
[2]W. Kaiser and C. D. Thurmond, J. Appl. Phys. **30**, 427 (1959).
[3]Y. Yatsurugi, N. Akiyama, Y. Endo, and T. Nozaki, J. Electrochem. Soc. **120**, 975 (1973).
[4]K. Sumino, I. Yonenaga, M. Imai, and T. Abe, J. Appl. Phys. **54**, 5016 (1983).
[5]H. J. Stein, Appl. Phys. Lett. **43**, 296 (1983).
[6]H. J. Stein, Appl. Phys. Lett. **47**, 1339 (1985).
[7]H. J. Stein, J. Electrochem. Soc. **132**, 668 (1985).
[8]H. J. Stein, in *Proceedings of the 13th International Conference on Defects in Semiconductors, Coronado, California, 1984,* edited by L. C. Kimerling and J. M. Parsey, Jr. (Metallurgical Society AIME, Warrendale, PA, 1985), p. 839.
[9]T. Abe, K. Kikuchi, S. Shirai, and S. Muraoka, in *Semiconductor Silicon 1981,* Proceedings of the 4th International Symposium on Silicon Materials Science and Technology, Minneapolis, edited by H. R. Huff (American Electrochemical Society, Pennington, NJ, 1981), p. 54.
[10]H. J. Stein, in *Oxygen, Carbon, Hydrogen, and Nitrogen in Crystalline Silicon,* edited by J. C. Mikkelsen, Jr., S. J. Pearton, J. W. Corbett, and S. J. Pennycook, MRS Symposia Proceedings No. 59 (Materials Research Society, Pittsburgh, 1986), p. 523.
[11]*Structure Reports,* edited by A. J. C. Wilson (International Union of Crystallography, Utrecht, 1951), Vol. 15, p. 341;

Vol. 16, p. 280.
[12]T. L. Cottrell, The Strength of Chemical Bonds (Butterworths, London, 1954), p. 279.
[13]J. B. Mitchell, P. P. Pronko, J. Shewchun, D. A. Thompson, and J. A. Davies, J. Appl. Phys. **46**, 332 (1975).
[14]R. Jones, S. Öberg, F. Berg Rasmussen, and B. Bech Nielsen, Phys. Rev. Lett. **72**, 1882 (1994). A preliminary report was given in F. Berg Rasmussen, B. Bech Nielsen, R. Jones, and S. Öberg, in *Proceedings of the 17th International Conference on Defects in Semiconductors, Gmunden, Austria, 1994,* edited by H. Heinrich and W. Jantsch (Trans Tech, Aedermannsdorf, 1994), p. 1221.
[15]L. C. Feldman, J. W. Mayer, and S. T. Picraux, *Materials Analysis by Ion Channeling* (Academic, New York, 1982).
[16]B. Bech Nielsen, Phys. Rev. B **37**, 6353 (1988).
[17]F. B. Hagedorn, and J. B. Marion, Phys. Rev. **108**, 1015 (1957).
[18]J. Lindhard, K. Dan. Vidensk. Selsk. Mat. Fys. Medd. **34**, 14 (1965).
[19]E. Bonderup, H. Esbensen, J. U. Andersen, and H. E. Schiøtt, Radiat. Eff. **12**, 261 (1972).
[20]D. S. Gemmell, Rev. Mod. Phys. **46**, 129 (1974).
[21]The estimation of the vibrational amplitude of the impurity is a well-known problem in channeling studies (Ref. 15). However, in this case the simulations depended only weakly on the amplitude and the contribution from this to the uncertainty in the nitrogen position is estimated to be about 0.1 Å.
[22]B. Bech Nielsen, J. U. Andersen, and S. J. Pearton, Phys. Rev. Lett. **60**, 321 (1988).
[23]F. Jensen, I. Stensgaard, F. Besenbacher, and K. Mortensen, Nucl. Instrum. Methods Phys. Res. Sect. B **48**, 334 (1990).
[24]E. F. Kennedy, B. Bech Nielsen, and J. U. Andersen, Nucl. Instrum. Methods Phys. Res. Sect. B **67**, 236 (1992).
[25]P. J. M. Smulders, D. O. Boerma, B. Bech Nielsen, and M. L. Swanson, Nucl. Instrum. Methods Phys. Res. Sect. B **45**, 438 (1988).
[26]Y. Itoh, T. Nozaki, T. Masui, and T. Abe, Appl. Phys. Lett. **47**, 488 (1985).

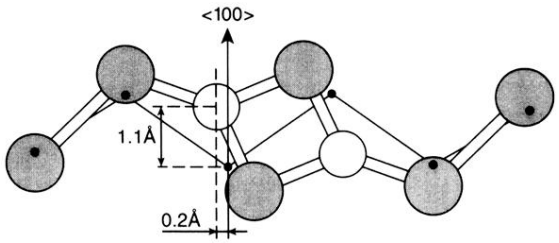

FIG. 10. Antiparallel model of the nitrogen pair defect (Ref. 14) shown in the $(01\bar{1})$ mirror plane (reproduced from Ref. 14). The small points mark the substitutional (perfect lattice) sites. Also indicated is the calculated (Ref. 14) displacement of the nitrogen atoms from the substitutional site.